Atomic de Broglie waves in multiple optical standing waves

Chang Jae Lee
Department of Chemistry, Sunmoon University, Asan 336-840, Korea
(Received 12 September 1995)

In this work the dynamical behavior of the center of mass of a two-level atom in sequences of multiple optical standing waves is explored. In a standing wave the atomic momentum distribution fans out. But with a suitably designed sequence of standing waves it is possible to refocus the momentum-space wave packet and bring the momentum distribution to the initial value, which may be regarded as an atom optical analog to spin or photon echo. If the total interaction time is fixed, the refocusing performance gets better as the number of standing waves in a sequence increases. Also the atomic wave packet in position space evolves as if in free space. [S1050-2947(96)03805-X]

PACS number(s): 03.75.Be, 42.50.Vk

I. INTRODUCTION

The manipulation of the external degrees of freedom, i.e., the center of mass, of atoms has grown into an immensely active field of atom optics [1]. Often the center-of-mass dynamics can be described in terms of classical trajectories. Such is the approach taken by McClelland *et al.* to account for their experiments on direct-writing atom lithography, the nanoscale deposition of atoms on a substrate by use of a laser [2]. But there are effects and applications that may be attributable only to the wave nature of the atoms. The wave nature becomes increasingly significant, for example, as the temperature of the atoms gets lower as in cooling experiments, and a full description of the wavelike behavior requires the use of quantum mechanics.

A well-known configuration to investigate various effects due to the wave nature of the atomic center of mass is the deflection of an atomic beam by a laser standing wave (SW). Recently, applications of the configuration but with two or more SW's were reported [3–6]. The goal of this work is to reveal a close analogy between the atom–multiple-SW interaction and coherent transient effects, especially the photon- or spin-echo phenomena. A SW is utilized also in schemes for atomic position measurement [7] or in depositing atoms on a substrate as in atom lithography [2,8]. In such experiments it is desirable to remove the motion of the atoms. Thus a simultaneous goal is to develop an all-optical method employing SW's for removing the transverse motion of the atoms.

The system under consideration is a beam of two-level atoms initially prepared with a narrow (coherent) momentum distribution. The atoms are then made to cross a sequence of optical SW's and the dynamical behavior of the atomic de Broglie waves is observed. An atomic beam is diffracted by a SW into components whose momenta are even multiples of the photon momentum (the Kapitza-Dirac effect), which was observed by Pritchard and co-workers [9]. The atomic momentum distribution spreads in the regime where the interaction time is short. Beyond the regime, however, the momentum spread undergoes a series of collapses and revivals [10], or Pendellösung-type oscillations [11]. Here we will limit discussions in the short-interaction-time regime. The SW provides spatial inhomogeneity to the atomic wave packet and the momentum spreading (and hence the loss of momentum coherence) is due to this inhomogeneity. The process is not irreversible, however, and the momentum coherence can be restored by a second, suitably chosen SW or a sequence of SW's. This may be considered as an atom optical analog to spin or photon echo, which involves a sequence of radio frequency or laser pulses, so we term it ''atom echo.'' While the echo technique developed by Chebotayev *et al.* [3] is concerned with spatial rephasing of an atomic beam, the schemes considered above work in momentum space. We also calculate the evolution of the atomic wave packet in the accompanying position space to see the effects of the schemes. In these calculations we integrate the time-dependent Schrödinger equation numerically, without using the usual Raman-Nath approximation.

The paper is organized as follows. In the next section a discussion is given on the evolution of the atomic wave packet in a SW in the Kapitza-Dirac regime, paying attention to the analogy with the precession of the Bloch vectors in the presence of spatial inhomogeneity. The analogy of the momentum refocusing with spin or photon echo is discussed in Sec. III. A comparison of refocusing performances of various SW sequences is also given in that section. The paper concludes with a summary of the main results in Sec. IV.

II. ATOM INTERACTING WITH A STANDING LIGHT WAVE IN A CAVITY

Consider a beam of two-level atoms moving along the z direction, which subsequently enters a cavity and interacts with a classical SW applied along the transverse direction (x direction). For large detunings spontaneous emission can be suppressed and the effective Hamiltonian for an atom is [12]

$$H=\frac{\mathbf{p}^2}{2m}+\frac{1}{2}\hbar\,\delta\omega\sigma_z+\hbar\,\frac{\Omega^2\cos^2(kx+\varphi)}{\delta\omega}\,\sigma_z, \qquad (1)$$

where m and $\mathbf{p}$ are the mass and the center-of-mass momentum of the atom and σ_z is a Pauli spin operator describing the population difference between the two internal states of the atom. $\delta\omega=\omega-\omega_0$ is the detuning between the atomic reso-

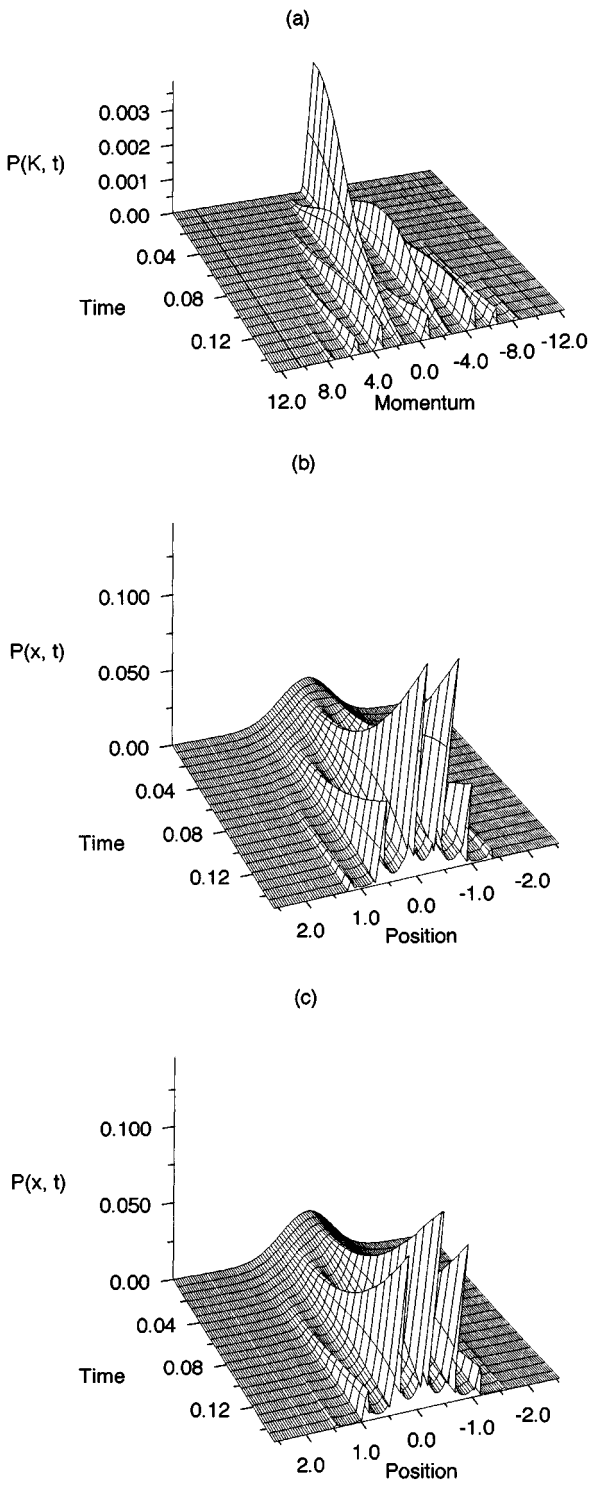

FIG. 1. Probability of finding an atom in a SW as a function of interaction time with $\delta\omega=1500$, $\Omega=300$, $\varphi=0$, and $t_{\rm int}=0.16$: (a) $P(K,t)$, in momentum space; (b) $P(x,t)$, in position space; and (c) in position space, but with $\delta\omega=-1500$ or $\varphi=\pi/2$. The frequencies and time are in units of respective recoil values of the atom. The momentum and position are in units of the momentum and wavelength of the SW field.

nance frequency ω_0 and the field frequency ω. The Rabi frequency is Ω and k and φ are, respectively, the wave vector and the phase of the SW.

The longitudinal component of the atomic momentum is unchanged in the course of interaction, so it suffices to consider only the transverse motion of the atom. It will be assumed that throughout the interaction the atom stays adiabatically in the ground state, which is initially given by a Gaussian wave packet

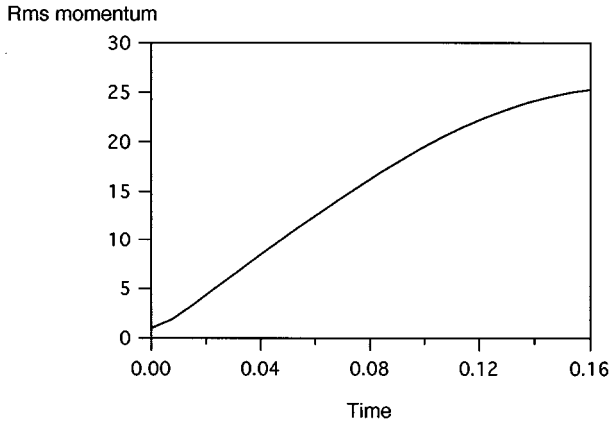

FIG. 2. rms momentum spread (in units of $\hbar k$) as a function of interaction time (in units of $t_{\rm rec}$) for the parameters of Fig. 1.

$$\psi(x,t=0)=(2\pi\sigma^2)^{-1/4}\exp\left[ik_0x-\left(\frac{x}{2\sigma}\right)^2\right], \tag{2}$$

where k_0 is the initial atomic wave vector and σ is the spread of atomic position. Thus we only have to solve the reduced one-dimensional Schrödinger equation for the ground state

$$i\hbar\,\frac{\partial}{\partial t}\,\psi(x,t)=H\psi(x,t), \tag{3}$$

where

$$H=\frac{p_x^2}{2m}+\hbar\,\frac{\delta\omega}{2}+\hbar\,\frac{\Omega^2\cos^2(kx+\varphi)}{\delta\omega}. \tag{4}$$

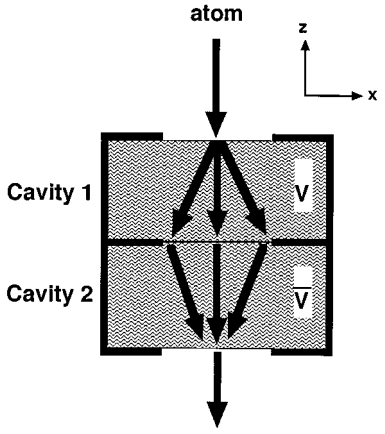

FIG. 3. Schematics of the two-SW sequence for momentum refocusing. V denotes the potential corresponding to the SW in cavity 1 and $\bar{V}$ the sign-reversed potential. The atom evolves in V for a period of $t_{\rm int}$ and then in $\bar{V}$ also for $t_{\rm int}$. The scheme will be called $V\bar{V}$ for simplicity.

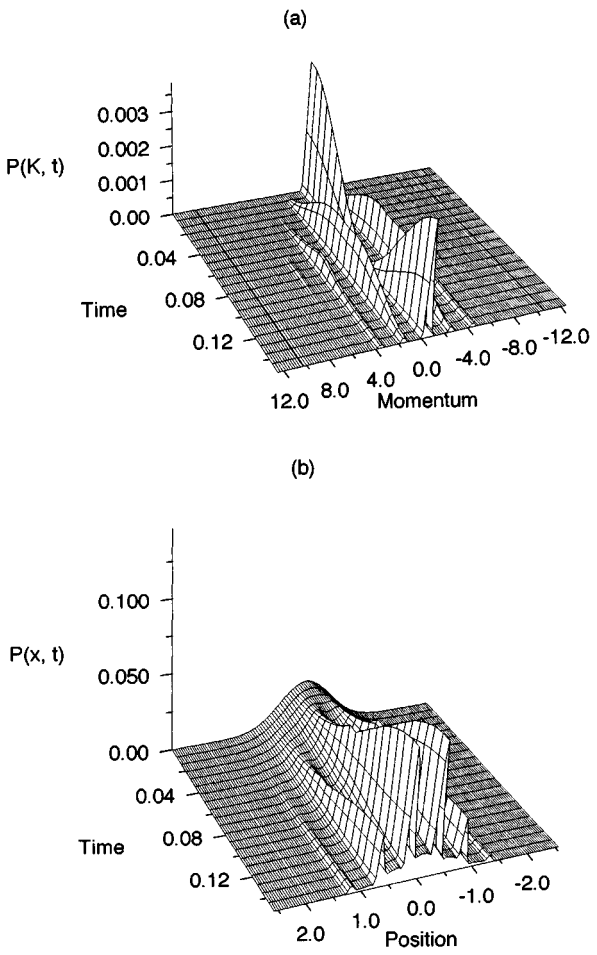

FIG. 4. (a) Momentum-space and (b) position-space probabilities as a function of interaction time for the two-SW sequence $V\overline{V}$ with $t_{\mathrm{int}}=0.08$ for each component SW. Other parameters are the same as in Figs. 1(a) and 1(b).

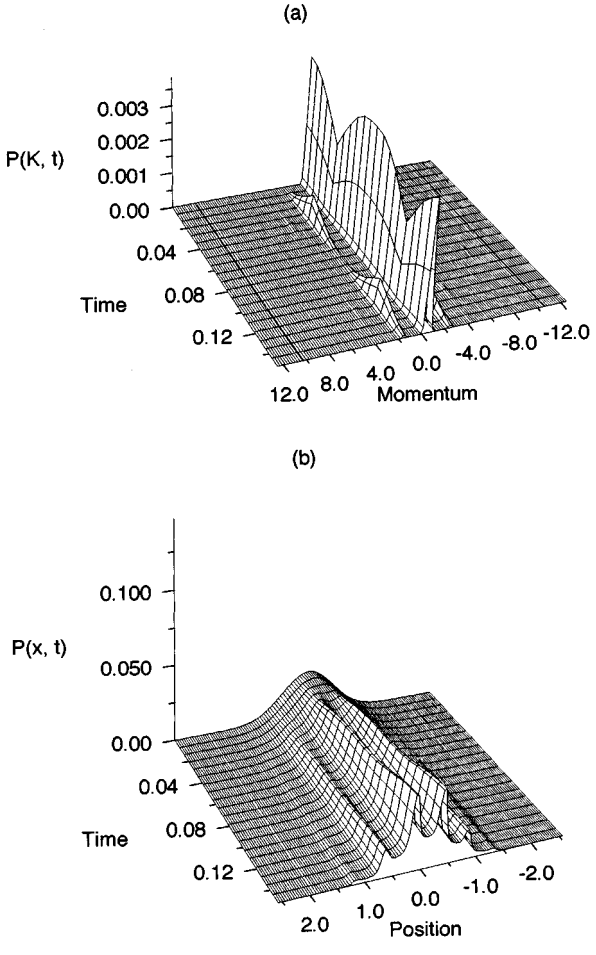

FIG. 5. Same as in Fig. 4 for the four-SW sequence $V\overline{V}V\overline{V}$ with $t_{\mathrm{int}}=0.04$ for each SW.

There is no known analytical solution to the above equation, so it has to be integrated numerically. In this work we employed both the Crank-Nicholson method as in Ref. [5] and the pseudospectral method [13]. Both methods gave no visible difference, but the former took much less computation time. If the kinetic-energy operator is ignored (the Raman-Nath approximation), which is valid for interaction times much shorter than the recoil time, the resultant solution is given by

$$\begin{aligned}\psi(x,t)&=\exp\left[i\left(\frac{1}{2}\,\delta\omega+\frac{\Omega^2}{2\,\delta\omega}\right)t\right]\exp\left[i\,\frac{\Omega^2 t}{2\,\delta\omega}\right.\\&\quad\left.\times\cos 2(kx+\varphi)\right]\psi(x,0)\\&=\exp\left[i\left(\frac{1}{2}\,\delta\omega+\frac{\Omega^2}{2\,\delta\omega}\right)t\right]\sum_{n=-\infty}^{\infty}i^n J_n\left(\frac{\Omega^2 t}{2\,\delta\omega}\right)\\&\quad\times e^{2in(kx+\varphi)}\psi(x,0).\end{aligned}\tag{5}$$

The second equality of Eq. (5) follows from the Jacobi-Anger identity (see, for example, Refs. [14, 15]). Likewise, the exact wave function $\psi(x,t)$ may be expanded in terms of plane waves modulated by the initial wave packet in the form

$$\psi(x,t)=\sum_{n=-\infty}^{\infty}c_n(t)\exp(ip_n x/\hbar)\psi(x,0),\tag{6}$$

where $p_n=n\hbar k$. A Fourier transform of $\psi(x,t)$ yields $\phi(p_x,t)$, which exhibits the near-field atomic (transverse) momentum distribution. Figure 1(a) shows as a function of interaction time t_{int} the probability $|\phi(p_x,t)|^2$ of finding momentum in units of photon momentum $\hbar k$.

The initial atomic Gaussian wave packet is assumed to have a width $\sigma=0.5$ (in units of optical wavelength λ) and $k_0=0$. From the uncertainty relation $\Delta x\Delta p=\hbar/2$ for a Gaussian wave packet one has the initial momentum spread $\Delta p=\hbar$ centered about zero. For convenience we introduce the recoil frequency ω_{rec} and the recoil time t_{rec} defined by $\omega_{\mathrm{rec}}=\hbar k^2/(2m)=1/t_{\mathrm{rec}}$. Then other parameters are $\delta\omega$ (in units of ω_{rec}), 1500; Ω (in units of ω_{rec}), 300; φ (in units of 2π), 0; and t_{int} (in units of t_{rec}), 0.16.

We see that as the interaction proceeds, the atomic momentum distribution fans out, giving rise to the well-known diffraction pattern that involves only integer multiples of $2\hbar k$. Although each diffraction process is coherent, the *overall* momentum coherence is lost because of the admixture of

TABLE I. Atomic rms momentum and position values for various standing-wave sequences (see the text for notations) at $t_{\rm int}=0.16$.

Sequence	$\Delta p/\hbar$	Δx
R	7.913 240 614 926 905 45	0.503 925 657 721 535 165
S	3.128 035 685 509 044 59	0.501 010 541 169 153 691
Q	1.690 932 654 971 640 02	0.500 149 584 574 719 074
$S\underline{S}$	1.692 068 295 072 820 33	0.500 291 382 516 725 094
$S\overline{S}$	1.107 309 984 298 619 28	0.500 070 496 767 292 066
$Q\underline{Q}$	1.102 580 576 941 442 43	0.500 056 039 550 526 377
QQ	1.099 618 696 330 666 87	0.500 051 827 940 291 846
$QQQQ$	1.026 157 196 583 899 15	0.500 050 137 745 488 153
$Q\overline{Q}QQ$	1.025 912 902 334 779 37	0.500 049 863 071 251 198
⋮	⋮	⋮
free-space values	1.000 000 000 000 000 00	0.500 065 697 970 206 690

partial waves with $p_n\neq 0$ in Eq. (6). To be more quantitative, the rms momentum spread as a function of $t_{\rm int}$ is shown in Fig. 2. This resembles the fanning out of Bloch vectors due to spatial inhomogeneity as they precess in the rotating frame, with subsequent loss of coherence. The spatial inhomogeneity for the atomic momentum decoherence mechanism is due to the optical SW, although the inhomogeneity is not completely random but periodic. Kurtsiefer *et al.* [16] recently reported the time-resolved experimental detection of momentum diffraction along with the rms momentum transfer for metastable helium atoms. The experimental results too show a linear growth of the rms momentum spread for short interaction times, which they explained in the context of the Raman-Nath approximation.

Although most studies on the atom-SW interaction concentrate on the momentum wave packet, it is also of interest how the position wave packet changes as a function of interaction time. The Raman-Nath solution given by Eq. (5) predicts that only the phase of the atomic wave packet changes as a result of the interaction with the SW. Without the Raman-Nath approximation, however, both the phase and the amplitude of the atomic wave packet are modulated, as discussed in Ref. [5]. Hence care has to be taken when one makes the (transmission) phase grating analogy to the SW. Figure 1(b) shows the dynamical localization of the initial Gaussian wave packet for blue detuning ($\delta\omega>0$) with $\varphi=0$ and Fig. 1(c) for red detuning with $\varphi=0$ (or blue detuning with $\varphi=\pi/2$). In the former case the wave packet localizes at the nodes of the SW, $\lambda/4$, $3\lambda/4$, $5\lambda/4$, . . . , where the potential minima are located, while for the latter case the wave packet localizes at the SW antinodes, $0,\lambda/2,\lambda,\ldots$.

III. REFOCUSING OF ATOMIC MOMENTUM

A. Refocusing with two SW's

If the interaction time is much longer than $t_{\rm rec}$ the momentum spread exhibits a series of collapses and revivals [10], or Pendelösung oscillations [11], if $k_0\neq 0$. However, one can reverse the process and make the momentum spread collapse within a time arbitrarily shorter than the collapse-revival period by a second SW with either an opposite sign of detuning or a $\pi/2$ phase shift. Either one of the parameters reverses the sign of the SW potential, which is analogous to applying a π pulse in coherent transient experiments. In this new environment the atoms with various momenta ''race backward'' and at $t=2t_{\rm int}$ they regroup. Let us denote V as the optical potential corresponding to the first SW with the parameters of Fig. 1 and V the sign-reversed potential. The dynamical refocusing of atomic momentum with the scheme VV depicted in Fig. 3, where the potentials are applied back to back, is shown in Fig. 4(a). For each potential the interaction time is taken to be equal to 0.08, so the total interaction time is again 0.16.

Note that the two SW regions touch in the scheme $V\overline{V}$. The free evolution period between the regions should degrade the refocusing performance. This is in contrast to the scheme of Ref. [3], in which the SW's are spatially separated. The resurrection of momentum coherence by applying two SW's is the aforementioned atom optical analog to spin or photon echo. The residual momentum spread at the end of the second SW is due to the kinetic-energy term in the Hamiltonian, the sign of which is not reversed by the scheme. The corresponding evolution of probability in position space is shown in Fig. 4(b).

B. Performance of multi-SW sequences

The refocusing performance can be improved with more SW's, e.g., $V\overline{V}\overline{V}V$, which corresponds to applying a sequence of two π pulses, which results in the formation of two echoes. Figure 5 shows the refocusing with the four-SW sequence and position-space probability. We take $t_{\rm int}=0.04$ for each component SW potential to give the same total interaction time. The performance improvement over the simple VV sequence is obvious.

It is rather easy to explain the performance improvement of a longer (in terms of the number of the VV unit) sequence. To that end let us rewrite the Hamiltonian in Eq. (4) as

$$H=\frac{p_x^2}{2m}+\hbar\,\frac{\Omega^2\cos 2(kx+\varphi)}{2\,\delta\omega}\equiv T+V, \tag{7}$$

where T and V denote the kinetic-energy and the potential-energy operators, respectively, and the constant terms have been dropped, since they have no dynamical effects. Let us

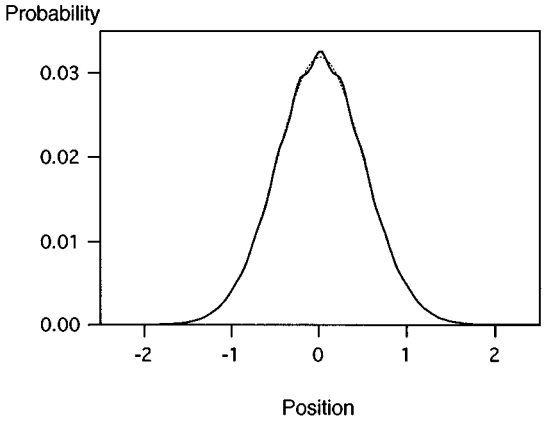

FIG. 6. Comparison of position-space wave packets. Dotted line, Gaussian wave packet evolved freely for $t=0.16$, solid line, in the 16-SW sequence $Q\overline{QQ}Q$ with $t_{\rm int}=0.01$ for each SW.

denote the evolution operator by U_+ (U_-), which corresponds to the potential V (V). The evolution operator for a time $\delta t\rightarrow 0$ may be split as

$$U_\pm=\exp\left[\frac{-i}{\hbar}(T\pm V)\delta t\right]\approx\exp\left(\frac{-i}{\hbar}T\delta t\right)\exp\left(\frac{\mp i}{\hbar}V\delta t\right)$$
$$\approx\exp\left(\frac{\mp i}{\hbar}V\delta t\right)\exp\left(\frac{-i}{\hbar}T\delta t\right), \tag{8}$$

which is accurate to first order in δt. Thus, within this degree of accuracy, if $\delta t=t_{\rm int}/2$,

$$U_+U_-=\exp\left(\frac{-i}{\hbar}T\delta t\right)\exp\left(\frac{-i}{\hbar}V\delta t\right)\exp\left(\frac{i}{\hbar}V\delta t\right)$$
$$\times\exp\left(\frac{-i}{\hbar}T\delta t\right)$$
$$=\exp\left(\frac{-2i}{\hbar}T\delta t\right)=\exp\left(\frac{-i}{\hbar}Tt_{\rm int}\right). \tag{9}$$

Therefore, the accuracy improves as the number of the $\overline{VV}$ unit increases in a sequence of fixed overall interaction time $t_{\rm int}$, and eventually as the number tends to infinity the atom moves as if it were in *free* space. In Table I the rms momentum and position spreads for various multiple-SW sequences are listed. We introduced the notation R for the $\overline{VV}$ unit and $S\equiv RR=\overline{VVVV}$ and $Q\equiv RR=V\overline{VVV}$. Indeed, as the sequence gets longer, the spreads converge to the free space values for a Gaussian wave packet [17]

$$(\Delta p/\hbar)_t=(\Delta p/\hbar)_0, \tag{10}$$

$$(\Delta x)_t=(\Delta x)_0\left\{1+\left[\frac{1}{2\pi(\Delta x)_0}\right]^4 t_{\rm int}^2\right\}^{1/2}, \tag{11}$$

which are 1.0 and 0.500 065 7, respectively, for the parameters $(\Delta x)_0=0.5$ and $t_{\rm int}=0.16$. The convergence of Δp is uniform. But Δx values of very long sequences are slightly less than that of the pure Gaussian wave packet, and as shown in Fig. 6 the behavior is due to the increased probability about the center.

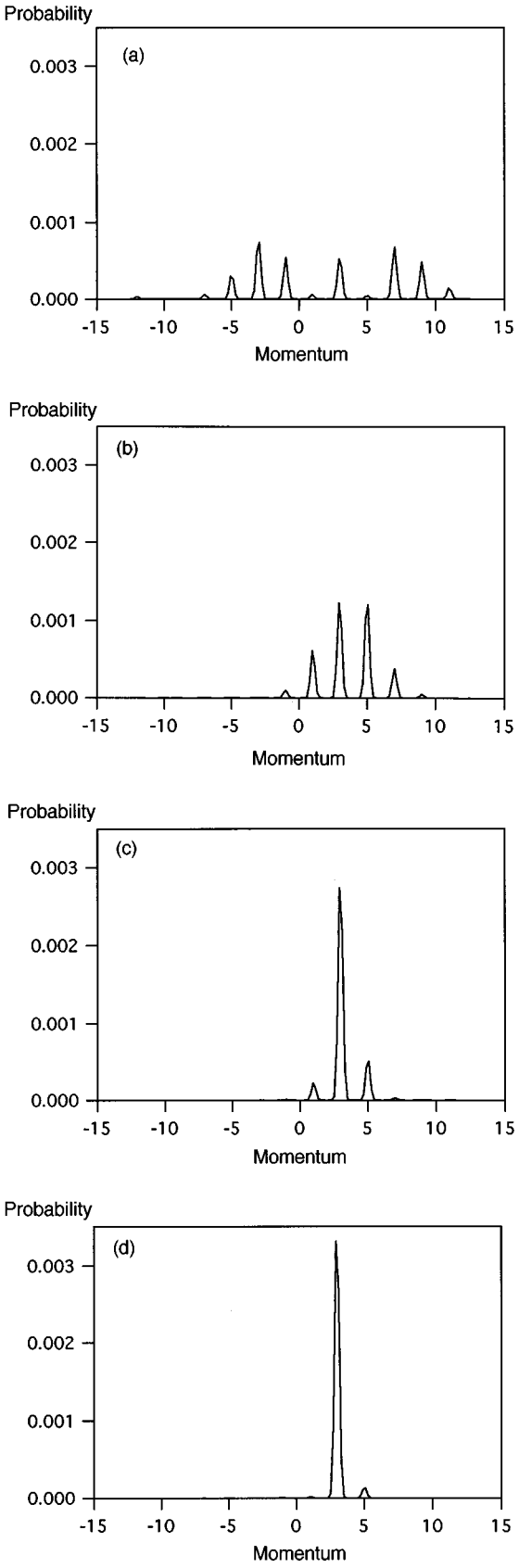

FIG. 7. Comparison of momentum distributions for various SW sequences with $k_0=3$: (a) V, (b) $\overline{VV}$, (c) $\overline{VVVV}$, and (d) $V\overline{VVV}$.

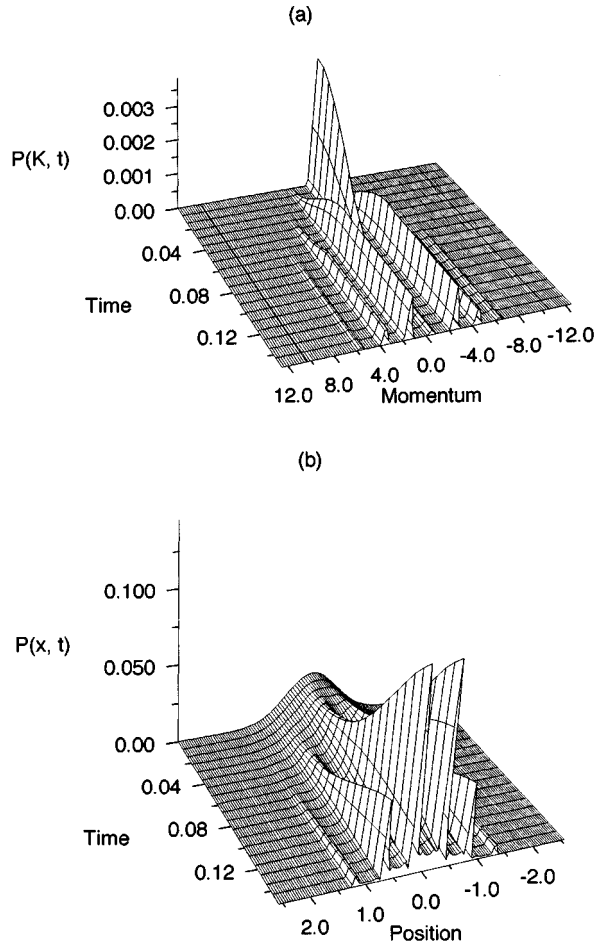

FIG. 8. (a) Momentum-space and (b) position-space probabilities as a function of evolution time for a SW with $t_{\text{int}}=0.08$ followed by a free evolution period $t_{\text{free}}=0.08$.

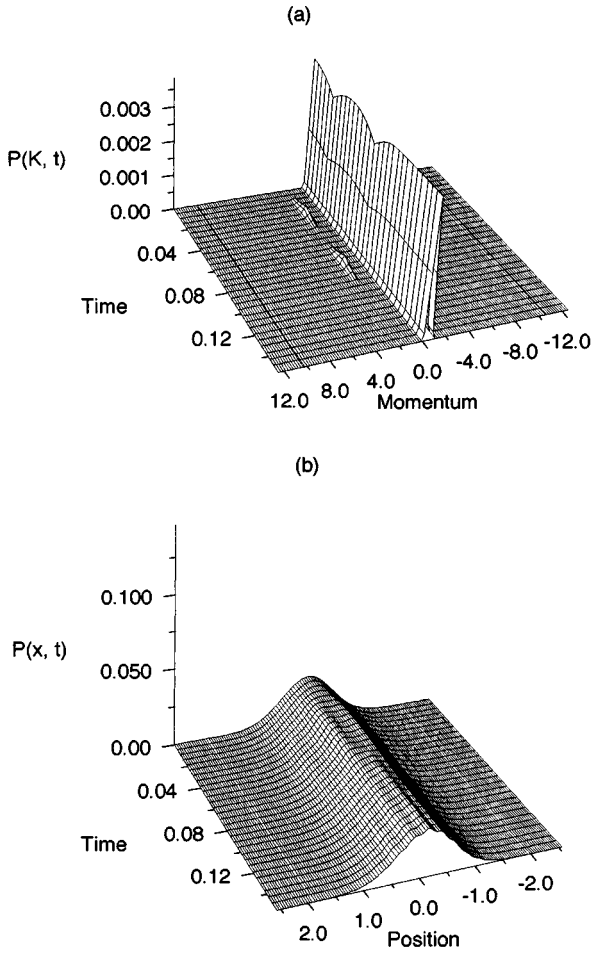

FIG. 9. Same as in Fig. 8 for the four-SW sequence $V\overline{VVV}$ with $t_{\text{int}}=0.02$ for each SW and $t_{\text{free}}=0.08$.

One may also note from Table I that there are substantial differences in refocusing performance among the sequences with the same length. For example, the rms momentum for the four-SW sequence Q is only half of that of S. Also, among the eight-SW sequences $QQ=R\overline{RRR}$ delivers the best performance. Moreover, the performance of the four-SW sequence Q is better than that of the eight-SW sequence SS. We note that both Q and QQ have the structure $W\overline{WWW}$ with $W=V$ and $W=R$, respectively.

The refocusing schemes work also for the nonzero initial momentum. Figure 7 shows refocusing of atomic momentum for $k_0=3$, keeping other parameters the same. Here too one finds the superior performance of the sequence $V\overline{VVV}$ over the $V\overline{VVV}$. Thus it appears that a sequence with a structure $W\overline{WWW}$ is highly efficient for refocusing.

C. Far-field momentum and position distributions

Thus far, we concentrated on the near-field evolution of the atomic wave packets. However, often measurements are made outside the cavity, where the atom evolves freely, so it is also of interest to investigate the far-field behavior of the atomic de Broglie waves. Figure 8 shows the localization as well as the momentum distribution with the SW on for $t_{\text{int}}=0.08$ followed by a free evolution period $t_{\text{free}}=0.08$, the total evolution time being also 0.16. As expected, no further momentum transfer to the atom occurs during the free evolution period. However, there is a substantial localization during the free evolution period, although the degree of localization is slightly less than that of Fig. 1(b). The continuation of the localization of the position wave packets after the SW is switched off is because of the fact that a certain portion of the atom possesses nonzero momentum as a result of a previous interaction with the SW. Hence, by removing the momentum it is possible to stop (or at least reduce) the localization during the free evolution period. Figure 9 shows the momentum and the position probabilities for the sequence $V\overline{VVV}$ applied for a period of 0.08 followed by a free evolution period of 0.08. As one can see, most of the momentum probability remains about the center (the zero momentum) and the localization is almost negligible during the free evolution period.

IV. SUMMARY

In this paper [18] we studied numerically the near- and the far-field transverse position and momentum distributions of a two-level atom in sequences of optical SW's. The sequences are designed to compensate the effects of an initial SW. So the linear growth of the rms momentum distribution and the localization of position that characterize the atomic

wave-packet dynamics in a SW are either reversed (the former) or reduced (the latter) with the sequences. The coherent refocusing of diffracted partial waves with different center-of-mass momenta bears an analogy to spin or photon echo. Such a coherent manipulation of atomic momentum may be beneficial in atomic position measurements or in atom lithography. The refocusing performance can be improved by increasing the number of SW's used, while keeping the total interaction time fixed.

ACKNOWLEDGMENT

This work was supported by Non-Directed Research Fund, Korean Research Foundation.

[1] For a recent review see C. S. Adams, M. Sigel, and J. Mlynek, Phys. Rep. **240**, 143 (1994).
[2] J. J. McClelland *et al.*, Science **262**, 877 (1993).
[3] V. P. Chebotayev *et al.*, J. Opt. Soc. Am. **2**, 1791 (1985).
[4] M. A. M. Marte and P. Zoller, Appl. Phys. B **54**, 477 (1992).
[5] P. A. Ruprecht, M. J. Holland, and K. Burnett, Phys. Rev. A **49**, 4726 (1994).
[6] B. Dubetsky and P. R. Berman, Phys. Rev. A **50**, 4057 (1994).
[7] For a recent review of precision position measurement of atoms see J. E. Thomas and L. J. Wang, Phys. Rep. **262**, 311 (1995).
[8] G. Timp *et al.*, Phys. Rev. Lett. **69**, 1636 (1992).
[9] For an overview of work on atom diffraction see D. E. Pritchard and B. G. Oldaker, in *Coherence and Quantum Optics VI*, edited by J. H. Eberly, L. Mandel, and E. Wolf (Plenum, New York, 1989), pp. 937–942.
[10] U. Janicke and M. Wilkens, Phys. Rev. A **50**, 3265 (1994).
[11] P. Meystre, E. Schumacher, and E. M. Wright, Ann. Phys. **48**, 141 (1991), and references therein.
[12] D. F. Walls and G. J. Milburn, *Quantum Optics* (Springer, Heidelberg, 1994), Chap. 17.
[13] See, for example, P. L. DeVries, *A First Course in Computational Physics* (Wiley, New York, 1994), Chap. 7.
[14] M. Born and E. Wolf, *Principles of Optics*, 6th ed. (Pergamon, Oxford, 1989), Chap. 8.
[15] R. J. Cook and A. F. Bernhardt, Phys. Rev. A **18**, 2533 (1978).
[16] Ch. Kurtsiefer, T. Pfau, C. R. Ekstrom, and J. Mlynek, Appl. Phys. B **60**, 229 (1995).
[17] E. Merzbacher, *Quantum Mechanics* (Wiley, New York, 1970), Chap. 8.
[18] A shorter version is to appear in *Coherence and Quantum Optics VII*, edited by J. H. Eberly, L. Mandel, and E. Wolf (Plenum, New York, in press).